

Electrical Properties of the V-Defects of Epitaxial HgCdTe

V.A. NOVIKOV ^{1,3} D.V. GRIGORYEV,¹ D.A. BEZRODNYI,¹
A.V. VOITSEKHOVSKII,¹ S.A. DVORETSKY,² and N.N. MIKHAILOV²

1.—Tomsk State University, 36, Lenina Avenue, Tomsk, Russia 634050. 2.— Institute of Semiconductor Physics, Siberian Branch, Russian Academy of Sciences, 13, Pr. Lavrentieva, Novosibirsk, Russia 630090. 3.—e-mail: novikovvadim@mail.ru

The manufacturing process of wide-band-gap matrix photodetector devices and miniaturization of their individual pixels gave rise to increased demands on the material quality and research methods. In the present paper we propose using the methods of atomic-force microscopy to study the local distribution of electrical properties of the V-defects that form in epitaxial films of *HgCdTe* during their growth process via molecular beam epitaxy. We demonstrate that a complex approach to studying the electrical properties of a predefined region of a V-defect allows one to obtain more detailed information on its properties. Using scanning spreading resistance microscopy, we show that, for a V-defect when the applied bias is increased, the surface area that participates in the process of charge carrier transfer also increases almost linearly. The presence of a potential barrier on the periphery of individual crystal grains that form the V-defect interferes with the flow of current and also affects the distribution of surface potential and capacitive contrast.

Key words: Kelvin force probe microscopy, molecular beam epitaxy, HgCdTe, fine films, contact potential difference

INTRODUCTION

At the present time, epitaxial layers of HgCdTe (MCT) are widely used for manufacturing high-performance components of infrared photoelectronics, especially matrix photodetector devices.¹ At the same time, in the MCT layers obtained by means of molecular beam epitaxy (MBE), the formation of macroscopic V-defects is observed without any relation to substrate type. The size of V-defects lies in the interval from 5 to 30 micrometers.^{2,3} In addition, it should be noted that these defects represent accumulations of microcrystal grains with the component composition different from that of the epitaxial film. In a number of papers, individual regions of V-defects have been reported to possess increased concentration of mercury, cadmium or tellurium.^{1–8} The variation of the component

composition of the local regions of a V-defect can lead to the formation of a complex potential profile.³ This, in turn, complicates the interpretation of the obtained measurement results of integral parameters of epitaxial MCT. For this reason knowing the distribution of the electrical properties of local V-defect regions would allow one to conduct a more adequate interpretation of the effects observed by means of other methods. Historically, the methods of photoluminescence, electron microscopy,^{2,6–8} x-ray structure analysis,⁵ and others were used to study the defects in MCT. However, presently there are just a few papers out on studying the electrical properties of such surfaces by means of atomic-force microscopy (AFM). In this work we demonstrate a complex approach to studying the properties of the surface of V-defects in epitaxial MCT using atomic-force microscopy. Such an approach allows to account for the fact that the presence of V-defects in epitaxial films and the electrical properties of these defects significantly impact the performance parameters of the large-format photodiode matrices based on p-n junctions.

MATERIALS AND METHODS

In the present work, we conducted a study of the electrical properties of the V-defects formed during the process of epitaxial growth of $Hg_{1-x}Cd_xTe$ films on GaAs (310) substrates. The composition of the upper variband layer on the surface was $x = 0.50$. The value of the parameter x as well as the thickness of the film were controlled by *in situ* ellipsometry measurements. Control over the composition x was carried out based on the optical transmission spectra at room temperature.

To study the electrical properties, we used the following methods of atomforce microscopy: Kelvin force probe microscopy (KPFM), scanning capacitance microscopy (SCM), and scanning spreading resistance microscopy (SSRM).

Kelvin force probe microscopy allows one to study the distribution of contact potential difference (CPD) (surface potential) between the cantilever needle-point and the surface.^{9–12} Because of the fact that the work function of the scanning probe does not change during the scanning process, one can obtain the distribution of the changes of the work function for the studied material by deriving it from the distribution of the surface potential. The spatial resolution of KPFM is at least 50 nm.¹³ It should also be noted that the KPFM is a two-pass technique,⁹ i.e., during the first pass the surface relief is examined and, then for the second pass, the needle is positioned at a certain distance z (about 10–100 nm⁹) above from the surface, and direct and alternating voltage is applied between the cantilever and sample which results in the appearance of an electrodynamic interaction force. During the second pass, the probe follows the surface relief at a distance z from the surface, which allows one to eliminate the influence of the sample morphology. In each scanning point the direct voltage is chosen in a way that secures that the interaction force between the cantilever needle-point, and the surface is equal to zero.

The main difference of the scanning capacitance microscopy from the KPFM is that the measurements of the electrodynamic interaction force are done using the second harmonic of the excitation signal.¹¹ This allows one to obtain the distribution of the change of capacity in the spacing between the cantilever needle-point and the surface. In other words, the SCM is a means for obtaining the capacitive contrast.

Scanning spreading resistance microscopy can be used to obtain the current strength distribution maps in the sample with an applied probe-sample fixed bias. Since the voltage does not change during the measurement process, the changes of the current strength reflect the non-uniform distribution of the sample resistance. In our studies of the V-defects in MCT, we obtained a number of AFM images for different voltage values at the needle, namely, for the interval from 0 to -10 V with a step of -1 V.

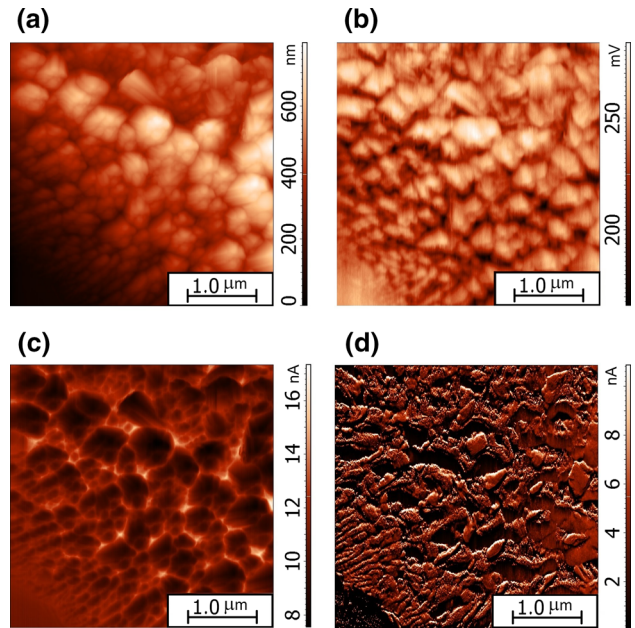


Fig. 1. AFM images of a MCT V-defect (a) surface morphology, (b) distribution of contact potential difference, (c) capacitive contrast, (d) spreading resistance.

The measurements were carried out at atmospheric pressure, room temperature, and ambient humidity below 35% by a commercial AFM “Solver HV” (NT-MDT, Moscow, Zelenograd). “Etalon HA HR/W2C+” probes produced by NT-MDT were used. Analogous measurements were performed in ultra-high vacuum at pressures about $0.5\text{--}1 \times 10^8$ Pa. The data show that the measurement results for the two cases lie within measurement error range. Taking into account that at room temperature $HgCdTe$ is a severely degenerated semiconductor, the adsorption film on its surface does not significantly affect the distribution of its electrical properties.

EXPERIMENTAL RESULTS

In this work by means of AFM we conducted a complex study of the electrical properties of the surfaces of V-defects of MCT epitaxial films. As mentioned above, these defects represent accumulations of individual microcrystal grains of MCT with the component composition different from that of the matrix.^{2–8} Figure 1 demonstrates typical AFM images of the surface morphology, distribution of contact potential difference, capacitive contrast and spreading resistance.

It can be seen from the AFM images presented in Fig. 1a that V-defects consist of microcrystal grains with a stretched shape and are approximately 150 nm in diameter. Close to the center of a V-defect these grains form large conglomerations with a mean diameter of about 500 nm. From the CPD distribution presented in Fig. 1b and taking into account the data from,¹¹ one can conclude that the grains forming a given defect possess a common

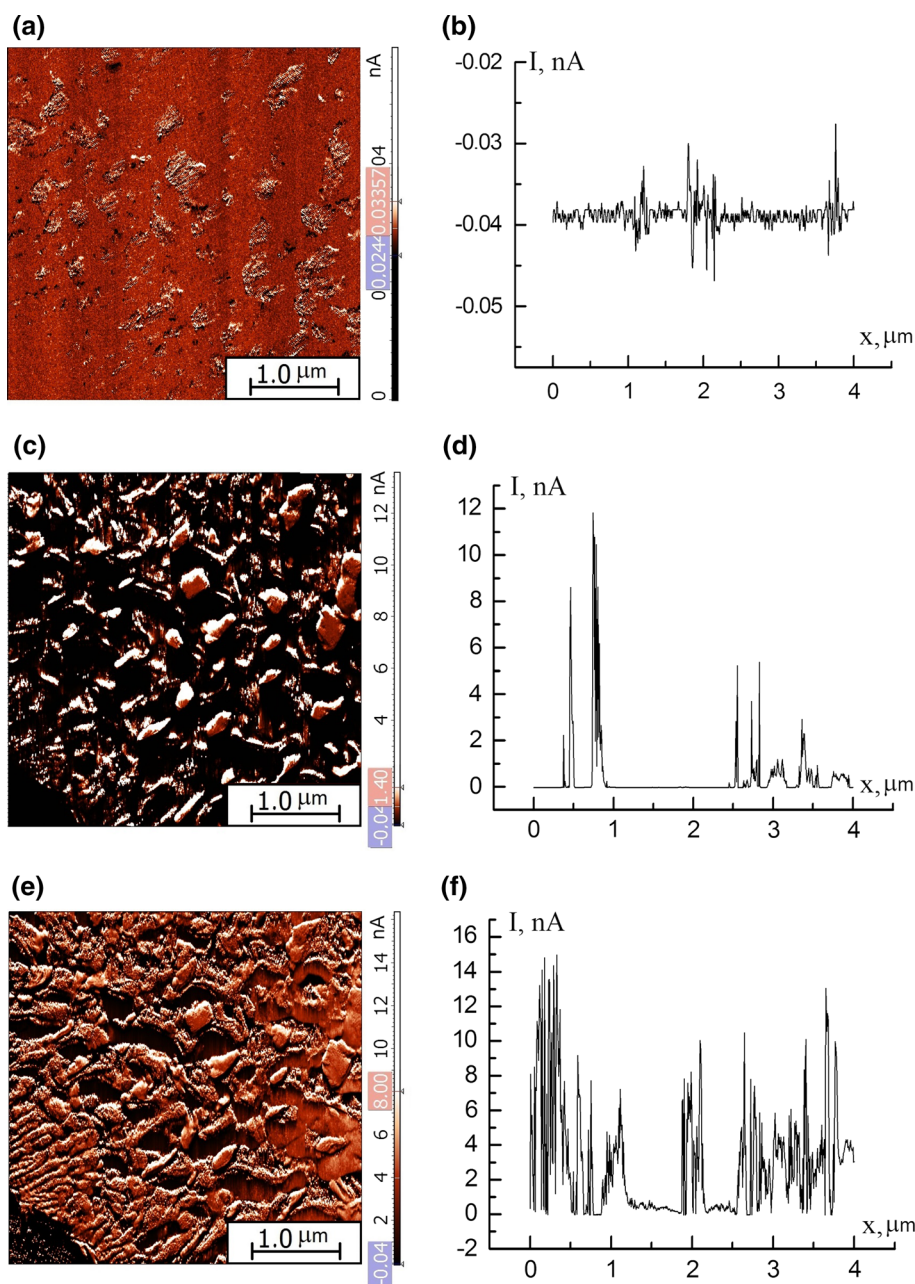


Fig. 2. AFM images of current strength distribution and their respective current distribution profiles for different voltage values: (a, b) 0 V, (c, d) -5 V, (e, f) -10 V.

preferred orientation. On the facets of individual microcrystal grains and their conglomerations, a change in the value of CPD is observed. This can be related either to the presence of an electric field that arises in between the lateral faces of the grains forming the defect, or to the influence of the changes of the crystallographic orientation of the lateral face.

From Fig. 1c one can see that along the periphery of microcrystal grains and their conglomerations there is a change of the capacity in the spacing between the cantilever needle-point and the surface. This indicates the presence of a charge in the near-

surface region of the microcrystal grains which should result in the formation of an additional bending of the energy band on the surface. In this case the changes in the process of the current flow on the periphery of the microcrystal grains is expected to occur which turns out to be in a good agreement with the data presented in Fig. 1d.

Figure 2 demonstrates AFM images of the distribution of the current strength under direct voltage at the needle. One can see that in the case of no external bias there is a flow of current through individual microcrystal grains. The presence of a number of separate regions with a non-zero current

strength with no external bias can be explained by the photocurrent induced by the red laser radiation diffraction on the cantilever beam. The laser mentioned here is used in AFM for the purposes of registering the working signal.

In case the external bias is secured, there is a gradual increase of the number of grains that contribute to the value of total current. An increased value of the current flowing through individual microcrystal grains is also observed. However, in this case there is no flow of current on the periphery of the grains which indicates the presence of a potential barrier, and the energy that is being supplied is not high enough so that the barrier can be overcome. The analysis of the area of the grains that contribute to the total current with respect to the supplied voltage showed that with the increase of the applied bias the electroconductive area of a V-defect also increases according to an almost linear law, up to 60% of the total studied area at -10 V.

Based on the data obtained for the value and distribution of the current along the V-defect area, one can conclude that in the presence of an external excitation the photocurrent flow will also be distributed non-uniformly along the defect. It should be mentioned that the presented measurements were conducted at room temperature when the semiconductor is highly degenerated. That is why we can assume that, under the working conditions (77 K) which are typical for the practical use of the devices, taking advantage of MCT-based structures the total V-defect area contributing to the value of the current can be different from the value obtained at a temperature of 300 K.

In conclusion, in the present paper it was shown that the electroconductive area of a V-defect of an epitaxial film increases when an external bias is secured. This increase obeys a nearly linear law, and reaches up to 60% of the total area. On the periphery of individual microcrystal grains and/or their conglomerations, there is also an additional

potential barrier that interferes with the charge carrier exchange. The presence of such a potential barrier significantly influences the distribution of the electrical properties of V-defects which can be seen from the results of measurements conducted by means of Kelvin force probe microscopy, scanning spreading resistance microscopy and scanning capacitance microscopy. The obtained data can be used in order to interpret the electrophysical properties of heteroepitaxial structures of MCT grown by means of MBE.

ACKNOWLEDGEMENTS

This study was supported by The National Research Tomsk State University competitiveness improvement programme in 2017.

REFERENCES

1. A. Rogalski, *Infrared Detectors* (Nauka, Novosibirsk, 2003).
2. E.V. Permikina, A.S. Kashuba, and V.V. Arbenina, *Inorg. Mater.* (2012). doi:[10.1134/S0020168512070126](https://doi.org/10.1134/S0020168512070126).
3. V.A. Novikov, D.V. Grigoryev, D.A. Bezrodnyy, and S.A. Dvoretzky, *Appl. Phys. Lett.* (2014). doi:[10.1063/1.4895573](https://doi.org/10.1063/1.4895573).
4. Y.G. Sidorov, S.A. Dvoretzky, V.S. Varavin, N.N. Mikhailov, M.V. Yakushev, and I.V. Sabinina, *Semiconductors* (2001). doi:[10.1134/1.1403569](https://doi.org/10.1134/1.1403569).
5. S.N. Yakunin and N.N. Dremova, *JETP Lett.* (2008). doi:[10.1134/S0021364008090099](https://doi.org/10.1134/S0021364008090099).
6. T. Aoki, Y. Chang, G. Badano, J. Zhao, C. Grein, S. Sivananthan, and D.J. Smith, *J. Cryst. Growth.* (2004). doi:[10.1016/j.jcrysgro.2004.01.063](https://doi.org/10.1016/j.jcrysgro.2004.01.063).
7. A.S. Kashuba, E.V. Permikina, and I.A. Nikiphorov, *Adv. Appl. Phys.* 1, 510 (2013).
8. T. Aoki, D.J. Smith, Y. Chang, J. Zhao, G. Badano, C. Grein, and S. Sivananthan, *Appl. Phys. Lett.* (2003). doi:[10.1063/1.1566462](https://doi.org/10.1063/1.1566462).
9. O. Vatel and M. Tanimoto, *J. Appl. Phys.* (1995). doi:[10.1063/1.358758](https://doi.org/10.1063/1.358758).
10. N.A. Torkhov and V.A. Novikov, *Semiconductors* (2009). doi:[10.1134/S106378260908020X](https://doi.org/10.1134/S106378260908020X).
11. W. Melitz, J. Shena, A.C. Kummel, and S. Lee, *Surf. Sci. Rep.* (2011). doi:[10.1016/j.surfrep.2010.10.001](https://doi.org/10.1016/j.surfrep.2010.10.001).
12. S.B. Kuntze, D. Ban, E.H. Sargent, St.J. Dixon-Warren, J.K. White, and K. Hinzer, *Crit. Rev. Solid State Mater. Sci.* (2007). doi:[10.1080/10408430590952523](https://doi.org/10.1080/10408430590952523).
13. H.O. Jacobs, P. Leuchtman, O.J. Homan, and A. Stemmer, *J. Appl. Phys.* (1998). doi:[10.1063/1.368181](https://doi.org/10.1063/1.368181).